Cyclotron resonance of electrons in surface space-charge layers on silicon

Gerhard Abstreiter,*† J. P. Kotthaus, and J. F. Koch
Physik-Department, Technische Universität München, 8046 Garching, Germany

G. Dorda
Forschungslaboratorium der Siemens AG München, 8 München, Germany

(Received 10 September 1975)

We study the high-frequency magnetoconductivity of the quasi-two-dimensional electron gas in a surface space-charge layer on Si. The experiments are carried out at low temperatures and in high magnetic field, using a far-infrared laser transmission spectrometer. Surface cyclotron resonance of electrons in inversion and accumulation layers on the (100) surface of Si has been investigated. The two dimensionality of the electron system is demonstrated by experiments in magnetic fields tilted with respect to the surface normal. Quantum oscillations are observed in the resonance amplitude, and are explained by a recent theory of Ando and Uemura. The resonance line shape is compared with the theoretical predictions. Scattering times, as extracted from the line shape, are related to those obtained from low-frequency conductivity experiments. The influence of a substrate bias voltage on the resonance is investigated. Subharmonic structure of the cyclotron resonance and its dependence on the surface charge density n_s are explored in the experiments. From the position of the fundamental resonance the cyclotron effective mass m_c^* is obtained. For $n_s \gtrsim 1\times10^{12}$ cm^{-2} and temperatures in the liquid-helium range we find $m_c^* = (0.197 \pm 0.005)m_0$ independent of n_s. For $n_s < 1\times10^{12}$ cm^{-2} a marked increase of m_c^* with decreasing n_s is observed. In some samples, and at $n_s \lesssim 0.5\times10^{12}$ cm^{-2}, a sample- and n_s-dependent decrease of the resonance field is found and interpreted as resulting from effects of localization. Results for electrons on (110) and (111) surfaces are also presented. The effect of multiple reflections in the semiconductor substrate on the transmission line shape of the surface cyclotron resonance is discussed.

I. INTRODUCTION

There is considerable current interest in electronic properties of space-charge layers on the surface of semiconductors.[1] Apart from their technological importance in semiconductor devices [the metal-oxide-semiconductor field-effect transistor (MOSFET)], space-charge layers are interesting physical systems. For a strong electric field, applied perpendicularly to the surface of a semiconductor, charge carriers are contained at the surface in a narrow channel (~50 Å). The number density of surface electrons n_s can be changed by varying the strength of the electric field, and is typically of order 10^{12} cm^{-2}. The electrons are bound in their motion normal to the surface in a one-dimensional potential well (Fig. 1), but they are free in their motion parallel to the surface. We have a quasi-two-dimensional electron gas.

Possible electron states in the potential well are the so-called electric subbands. Solving Schrödinger's and Poisson's equation self-consistently, one gets the energy eigenvalues of the system.[1] The total energy is given by

$$E_i(k_x,k_y) = E_i + \hbar k_x^2/2m_x + \hbar k_y^2/2m_y, \qquad (1)$$

where E_i is the energy at the bottom of the ith electric subband. In the simplest approximation, using a triangular potential well, one gets the eigenvalues $E_i \propto (m_\perp)^{-1/3}$, where $m_\perp$ is the effective mass perpendicular to the surface. For the (100) surface of Si, one has two sets of inequivalent valleys; one with $m_\perp = 0.916m_0$ (twofold degenerate) and one with $m_\perp = 0.1905m_0$ (fourfold degenerate).[2] The lowest-lying electric subband is the one with the heavy mass normal to the surface. In this case the mass for the motion parallel to the surface is $m_x = m_y = 0.1905m_0$. Under the usual experimental conditions only this lowest electric subband is occupied, one is in the so-called electric quantum limit. The density of states of the two-dimensional electron gas is independent of energy and given as

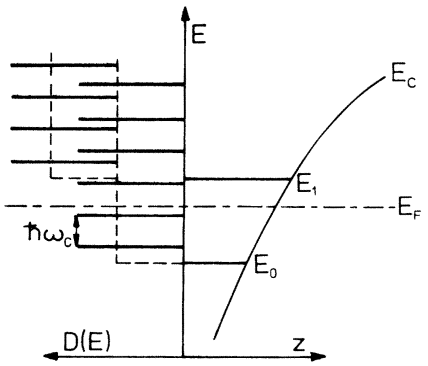

FIG. 1. Schematic representation of the conduction-band edge E_c and subband levels E_0, E_1. On the left-hand side are shown the density-of-states function $D(E)$ and Landau levels.

$$D(E) = g_s g_v (m_x m_y)^{1/2}/2\pi\hbar^2, \quad (2)$$

where g_s and g_v are the spin and valley degeneracies, respectively. A magnetic field, applied perpendicularly to the surface, quantizes the parallel motion. The energy eigenvalues are then given by

$$E_{ni} = E_i + (n+\tfrac{1}{2})\hbar\omega_c \pm \tfrac{1}{2} g \mu_B H, \quad (3)$$

where n is the Landau-level index, $\omega_c = eH/m_c^* c$ is the cyclotron frequency at the magnetic field H, and the last term describes the spin splitting. The density of states becomes discrete; the number of states per Landau level is

$$D(E)\hbar\omega_c = g_s g_v eH/2\pi c\hbar = g_s g_v/2\pi l_0^2, \quad (4)$$

where $l_0 = (c\hbar/eH)^{1/2}$ is the radius of the first Landau level.

Extensive investigations of the electronic properties in surface space-charge layers have been carried out in the past decade. To date there have been primarily studies of static properties such as conductivity, capacitance, tunneling, and piezoresistance.[1] The aim of the present work is to probe the space-charge layer with high-frequency cyclotron-resonance (CR) experiments. Such studies of the dynamical conductivity parallel to the surface provide essential new information. The cyclotron effective mass m_c^* and the scattering time τ can be determined independently. In addition, one expects to observe effects of the complete quantization of the system and other properties characteristic of the quasi-two-dimensional electron gas.

From transport measurements it is known that the scattering time τ of electrons in an inversion layer is of order 10^{-12} sec.[3] To satisfy the condition $\omega\tau > 1$, CR experiments have to be performed at far-infrared frequencies (~1000 GHz). For the (100) surface of Si, we expect an effective mass $m_c^* \approx 0.2 m_0$. The magnetic field H required for resonance is of order 10 T. The cyclotron radius for surface electrons is about 100 Å. The observation of such far-infrared CR in Si has recently been reported in the literature.[4-7]

In Sec. II, we first discuss the theoretical aspects of the CR line shape for a two-dimensional electron gas. After the description of the experimental necessities and problems in Sec. III, follows a detailed discussion of the various experimental observations in Sec. IV.

II. THEORETICAL CONSIDERATIONS

In a strong magnetic field the energy spectrum of the surface electron system is discrete and one cannot expect the classical description of CR to be valid. Ando and Uemura[8,9] have given a theory of CR in the two-dimensional electron gas. This theory is based on earlier calculations of the static magnetoconductivity.[10] Scattering is described in the lowest Born approximation and the resulting broadening is included in a self-consistent way in the density-of-states function $D(E)$. This leads to a semielliptic density-of-states profile of each Landau level, i.e.,

$$D(E) = \frac{1}{2\pi l_0^2}\,\frac{2}{\pi\Gamma_n^2}\left[1 - \left(\frac{E-E_n}{\Gamma_n}\right)^2\right]^{1/2}, \quad (5)$$

in which $2\Gamma_n$ is the width of the nth Landau level. CR absorption is related to the dynamical conductivity $\sigma_{xx}(\omega, H)$. The latter is numerically evaluated for different scattering potentials.

For short-range scatterers $d \ll l_0$ (d is the range of the scatterers) and $\omega_c\tau \gtrsim 2$, the width of each Landau level is independent of the quantum number n and is given by

$$\Gamma_n = \Gamma \approx \left(\frac{2}{\pi}\hbar\omega_c\frac{\hbar}{\tau_0}\right)^{1/2} \propto \left(\frac{H}{\tau_0}\right)^{1/2}, \quad (6)$$

where τ_0 is the scattering time at $H = 0$. The width of the resonance line, in a sweep of frequency at constant H, is determined by the width of the Landau levels. It is proportional to $(H)^{1/2}$. All transitions from filled states to adjacent empty states are allowed. The broadening caused by short-range scatterers is called the homogeneous or lifetime broadened case.

In the theory the maximum of $\mathrm{Re}\sigma_{xx}(\omega, H)$, and the related CR absorption, depends on the position of the Fermi energy E_F with respect to the Landau levels. If E_F lies between two adjacent Landau levels (filled case), the resonance is symmetric around $\omega = \omega_c$. If E_F lies in the center of a given Landau level (half-filled case), the resonance maximum is shifted to higher frequency $\omega > \omega_c$. The dependence of the resonance absorption on the position of the Fermi level causes quantum oscillations in surface CR if one sweeps the magnetic field at fixed frequency through the resonance. The oscillations are characteristic of the complete quantization in two dimensions.

For scatterers with long-range potentials $d \gg l_0$, the so-called inhomogeneous broadening, the level width will be determined by the potential variations. It is found to depend on the Landau quantum number, such that $\Gamma_{n-1} > \Gamma_n > \Gamma_{n+1}$. For inhomogeneous broadening, the selection rule for transitions between two neighboring Landau levels is more restrictive. The width of the resonance line is determined by the difference in the width of the neighboring Landau levels ($\sim \frac{1}{2}|\Gamma_n - \Gamma_{n+1}|$). Except for the magnetic quantum limit, the position of the resonance maximum is not dependent on the position of the Fermi ener-

gy with respect to the Landau levels. One should not expect to observe quantum oscillations in the case of scatterers with long-range potentials.

Ando's calculations scan the spectrum of scattering potentials also through the intermediate $d \sim l_0$ range. He gives numerical results that can, however, not be as easily described as the two limiting cases.

III. EXPERIMENTAL ASPECTS

Surface CR is studied in the transmission arrangement shown in Fig. 2. The transmission of far-infrared radiation at fixed frequency is observed as a function of magnetic field. The radiation is provided by molecular gas lasers operating at a number of discrete wavelengths in the far infrared. For most measurements the 337-μm (890.7 GHz) HCN line was used. Some experiments made use of the 220-μm H_2O and the 195-μm DCN lines.

The far-infrared radiation is focused with a copper cone onto a sample area 2 mm in diameter. The transmitted intensity is detected by a Ga-doped Ge bolometer. The magnetic field H is generated either by a 10-T superconducting solenoid or a 15-T Bitter solenoid. Two different methods of measurement are used. To measure direct transmission the incident laser beam is chopped at a frequency of about 10 Hz. Derivative transmission data are obtained by modulating the magnetic field at about 3–6 Hz with amplitudes up to 0.4 T peak to peak.

The samples are metal-oxide-semiconductor (MOS) capacitors on Si substrates of nominal 10-Ω cm material. The oxide layer thickness is ~2000 Å. A thin (~30 Å, $R_\square \sim 1\text{k}\Omega$), semitransparent layer of a NiCr alloy serves as a gate electrode. The samples are not provided with the usual source and drain contacts. The surface layer is charged through the substrate, using a contact on the back side of the sample. Since Si is an insulater at He temperatures, carriers have to be generated by illuminating the sample with radiation for which $\hbar\omega > \epsilon_g$, the band-gap energy. This light enters the sample light pipe through a 45° metallic wire mesh. After charging the surface layer the light is removed. The sample temperature can be varied in the range 2–80 °K and is measured with a capacitance thermometer.

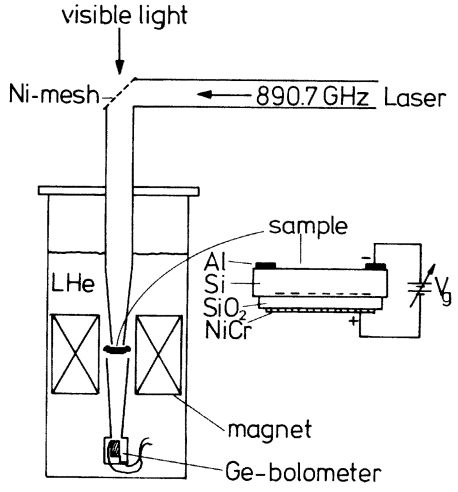

FIG. 2. Experimental arrangement for transmission CR experiments.

Several methods are employed to characterize the sample. The oxide thickness is measured with an ellipsometric method to an accuracy of ±10 Å. From capacitance-voltage measurements we determine the inversion threshold and impurity concentration. Microwave conductivity experiments are used to measure mobility, the scattering time τ, and to observe Shubnikov-de Haas oscillations.[11] From the latter we establish the relation between gate voltage V_g and the density n_s in the lowest subband.

To interpret the experimental results we have to relate the transmitted intensity to the dynamical conductivity $\sigma_{xx}(\omega, H)$. In terms of the ± circularly polarized conductivities $\sigma_{xx}(\omega, H) = \frac{1}{2}(\sigma^+ + \sigma^-)$. We consider the case of radiation with wavelength λ incident perpendicularly on a nonabsorbing, plane-parallel dielectric slab of refractive index n (i.e., the Si substrate), which on one face has an infinitely thin layer with conductivity $\sigma_{xx}(\omega, H)$ (i.e., the space-charge layer). As discussed in the appendix, interference effects will, in general, distort the line shape. For the special case where the substrate thickness d is a multiple of $\lambda/2n$, which at 337 μm is realized for many of our samples, one obtains for circularly polarized radiation the normalized power transmission $T^\pm$, reflection $R^\pm$, and absorption $A^\pm$ as

$$T^\pm = 4/|2+F^\pm|^2, \quad R^\pm = F^{\pm 2}/|2+F^\pm|^2, \quad A^\pm = 4F^\pm/|2+F^\pm|^2, \tag{7}$$

where $F^\pm = (4\pi/c)\sigma^\pm(\omega, H) = (4\pi/c)(n_s e^2 \tau/m^*) S^\pm(\omega, H)$. $S^\pm(\omega, H)$ is a normalized resonance line-shape function, classically given by $S^\pm(\omega, H) = [1 - i(\omega \mp \omega_c)\tau]^{-1}$. For the two-dimensional electron gas quantum-mechanical calculations of $S^\pm(\omega, H)$ have been carried out by Ando.[9]

It is instructive to compare the conductivities according to various different models. In Fig. 3 are given two examples for different values of n_s and τ_0, the relaxation time in the absence of a magnetic field. The dotted curve gives the quantum-mechanical result. For an overall, approx-

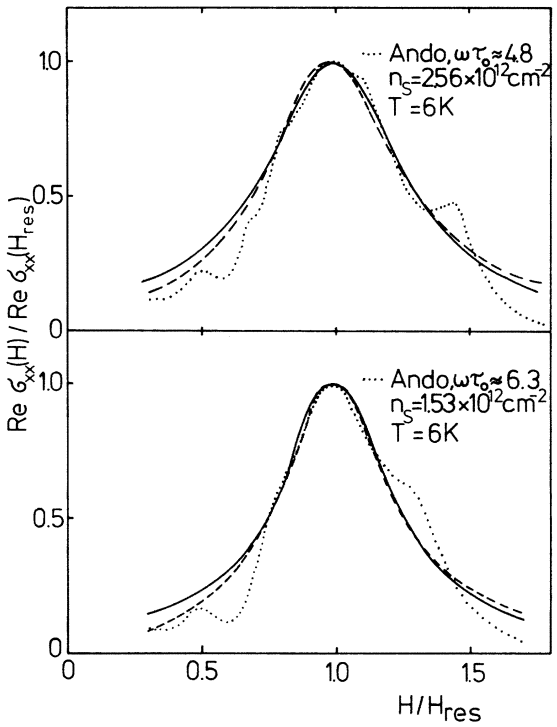

FIG. 3. Real part of the dynamical magnetoconductivity $\sigma_{xx}(\omega,H)$ according to Ando (dotted line) and in the classical approximation [solid line, constant $1/\tau$; dashed line, $1/\tau = (1/\tau_{res})\,(H/H_{res})^{1/2}$]. The classical fit requires $\omega\tau_{res} = 3.3$ and 4 for the upper and lower curves, respectively.

imate description of the resonance line one may use the classical conductivity expression using a different value of the relaxation time. A good fit is achieved with the solid lines using $\omega\tau_{res} = 3.3$ and 4 in the two curves. τ_{res} has the meaning of a scattering time at the resonance field H_{res}. For $\omega_c\tau > 2$ one may include the theoretically predicted $(H)^{1/2}$ dependence of the scattering rate in the classical expression by replacing $1/\tau$ with $(1/\tau_{res}) \times (H/H_{res})^{1/2}$. The result is the dashed line in Fig. 3. In the classical description of the conductivity there is very little difference in the linewidth and position of the resonance between the constant $1/\tau$ and $1/\tau \propto (H)^{1/2}$ version for $\omega\tau \gtrsim 3$.

In the limit of small signals ($\max|F| \ll 2$) Eq. (7) can be simplified. For the case of linearly polarized radiation one obtains

$$T = \tfrac{1}{2}(T^+ + T^-) \approx 1 - \mathrm{Re}F = 1 - (4\pi/c)\,\mathrm{Re}\sigma_{xx}(\omega,H), \qquad (8)$$
$$A = \tfrac{1}{2}(A^+ + A^-) \approx \mathrm{Re}F = (4\pi/c)\,\mathrm{Re}\sigma_{xx}(\omega,H).$$

The change in transmitted intensity becomes directly proportional to $\mathrm{Re}\sigma_{xx}(\omega,H)$. For low densities n_s, and not too high values of τ, this limit applies in Si. We estimate with $n_s = 1\times10^{12}$ cm^{-2}, $\tau = 3\times10^{-13}$ sec, and $m_c^* = 0.2m_0$ an absorption signal A of order 8% at 891 GHz. For this case one can directly compare of the experimentally observed signal with $\mathrm{Re}\sigma_{xx}(\omega,H)$. At higher values of ω or τ Eq. (7) has to be used.

In Table I are listed some of the relevant properties of samples used in the experiments.

IV. RESULTS AND DISCUSSION

The aim of this work is the determination of the effective mass m_c^* and the scattering time τ of electrons in surface space-charge layers on Si. The two-dimensional character of the system has a marked influence on the CR. In Fig. 4 we show an example of the change in the transmitted power $P(H)$, as well as its derivative dP/dH, observed in a Si(100) inversion layer at $T \simeq 5$ K, $f = 890.7$ GHz and $n_s \simeq 1.5\times10^{12}$ cm^{-2}. At low temperatures and $n_s \gtrsim 1\times10^{12}$ cm^{-2} we typically find quantum oscillations in the resonance amplitude (arrows in Fig. 5). In addition, subharmonic structure appears at the low-field side of the resonance. The linewidth is found to depend on the electron density and on substrate bias. The line shape shows a broadening on the high-field side. For

TABLE I. Sample characteristics. ρ is the nominal substrate resistivity; d_{ox} the oxide thickness (±10 Å); d the measured substrate thickness (±1 μm). y is the interference parameter discussed in the Appendix.

No.	Substrate	Surface	ρ (Ω cm)	d_{ox} (Å)	d (μm)	$y(\lambda = 337\ \mu m)$
A 1–3	*p* type	(100)	~ 10	2010	250	0.02
D 1–7	*p* type	(100)	8	2330	348	0.99
E 1–3	*p* type	(100)	100	1700	198	0.98
W 1–9	*p* type	(100)	6	2230	353	0.09
S 1–3	*p* type	(100)	6	2230	367	0.37
B 1–4	*n* type	(100)	~ 12	2400	284	0.71
C 1–3	*n* type	(100)	~ 2	2330	191	0.84
F 1–3	*p* type	(110)	?	2250	219	0.40
H 1–4	*n* type	(111)	100	2300	204	0.10

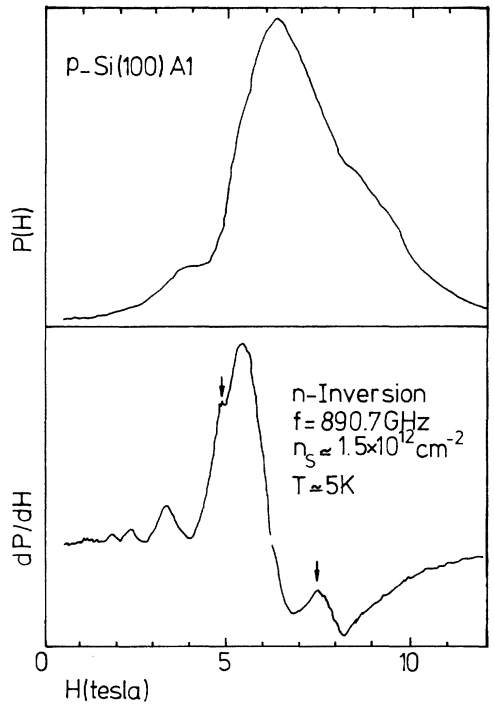

FIG. 4. Surface CR in sample $A1$. $P(H)$ is the change in transmitted intensity. Quantum oscillations are marked with arrows in dP/dH. The oscillations below the resonance are subharmonics.

$n_s \lesssim 1\times10^{12}$ cm^{-2} the resonance position depends on the electron density. In Secs. IV A–IV F we will discuss in detail the various results obtained for electrons in inversion and accumulation on the (100) surface of Si. In Sec. IV G we present results for electrons on (110) and (111) surfaces of Si.

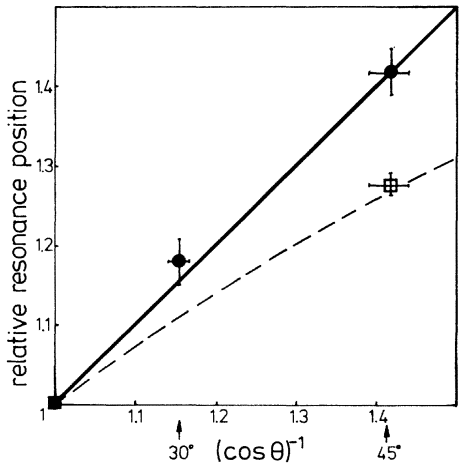

FIG. 5. Relative position of surface CR in sample $A1$ vs the reciprocal of the cos of the tilt angle θ. The dashed line gives the result for volume CR.

A. Tilted field experiments

Our first concern is to show that the surface charge layer is a two-dimensional system. To do this, we observe CR in a magnetic field tilted by an angle θ away from the surface normal. One expects a shift of the resonance to higher magnetic fields according to $(\cos\theta)^{-1}$, as long as the binding energy perpendicular to the surface is larger than the magnetic energy. The tilt experiments indeed show the resonance to shift to higher magnetic fields. Results for $\theta = 0°$, 30°, and 45° are plotted in Fig. 5. The solid line indicates the expected shift according to $(\cos\theta)^{-1}$. The dashed line gives the experimentally observed increase of m_c^* from microwave-frequency volume CR measurements.[12] The two points entered at 0° and 45° give our result for the volume resonance at 890.7 GHz. The $(\cos\theta)^{-1}$ dependence of surface CR was confirmed for n_s between 0.2×10^{12} and 4×10^{12} cm^{-2} in an inversion layer. According to the work of Kneschaurek *et al.*,[13] even at the lowest density of 0.2×10^{12} cm^{-2}, the subband energy separation is about 10 meV. This is substantially more than the magnetic energy $\hbar\omega_c$, which at resonance is 3.7 meV.

B. Quantum oscillations

A characteristic of surface CR is the quantum oscillations which appear at low temperatures and sufficiently high n_s. Some examples are shown in Fig. 6. This type of oscillation is observed in both inversion and accumulation layers. A comparison of the experimental results with Ando's quantum-mechanical calculations gives satisfactory agreement (Figs. 6 and 7). The dotted theoretical curves give the real part of the conductivity $\sigma_{xx}(\omega,H)$. Strictly speaking, such a comparison is valid only in the small signal limit and when interference effects can be neglected. Interference can safely be ignored for samples $A1$ and $D3$, but the signals in Figs. 6 and 7 do not qualify as small. The calculations of $\mathrm{Re}\sigma_{xx}(\omega,H)$ do not give quantitatively correct the amplitude, linewidth, and shape of the resonance. The quantum oscillations are described satisfactorily by the calculation.

The oscillations are caused by a modulation of the resonance amplitude as the Landau levels move through the Fermi level. These oscillations are not the Shubnikov–de Haas oscillations observed in static conductivity measurements. The quantum oscillations vanish at high magnetic fields above the CR line. They appear only within the region of the CR, because they arise from a variation in the resonance amplitude. The oscillations

vanish, if the width of the Landau levels Γ_n is much smaller than their separation $\hbar\omega_c$. They are strongest at some finite ratio $\hbar\omega_c/\Gamma_n$. At resonance ($\omega=\omega_c$) the oscillations vanish and reverse their phase. When the Fermi energy lies in the center of a Landau level, one gets maximum absorption for $\omega_c<\omega$, a minimum for $\omega_c>\omega$. This is evident from the arrows marked in Fig. 6.

The oscillations are periodic in reciprocal field, and the period is a measure of the electron density n_s. This allows one to obtain directly a value of the carrier density at each gate voltage. In Fig. 7 are given the values of n_s used in the calculation. A comparison of the curves shows that in a favorable case the density n_s can be obtained with an accuracy of a few percent. The amplitude of the experimentally observed oscillations is always less than the predicted one. This could be due in part to inhomogeneous broadening of the Landau levels. Ando points out[9] that the oscillations appear only in the case of short-range scattering.

As in Fig. 8, the quantum oscillations vanish with increasing temperature. At $T\sim 21$ K no os-

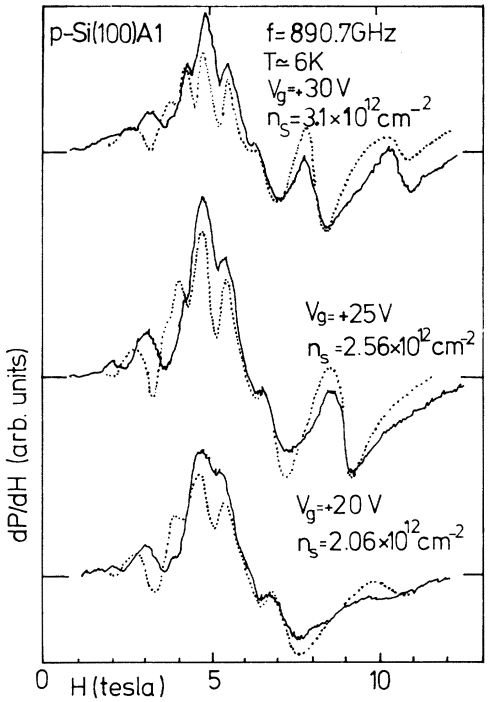

FIG. 7. Comparison of the derivative signals dP/dH with $d\,\mathrm{Re}\sigma_{xx}(\omega,H)/dH$ according to Ando. n_s gives the density used in the calculation. The structure below 3 T in theory and experiment is the subharmonic resonance.

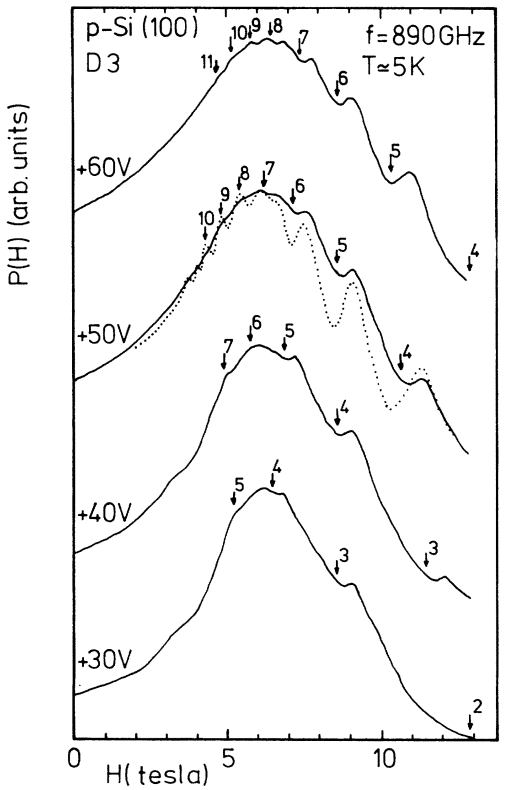

FIG. 6. CR signals for high electron densities (at 10 V the electron density is approximately 0.9×10^{12} cm^{-2}). The arrows mark the field, where E_F lies in the center of the nth Landau level. The dotted curve is Ando's result of $\mathrm{Re}\sigma_{xx}(\omega,H)$ for $n_s=4.4\times10^{12}$ cm^{-2}.

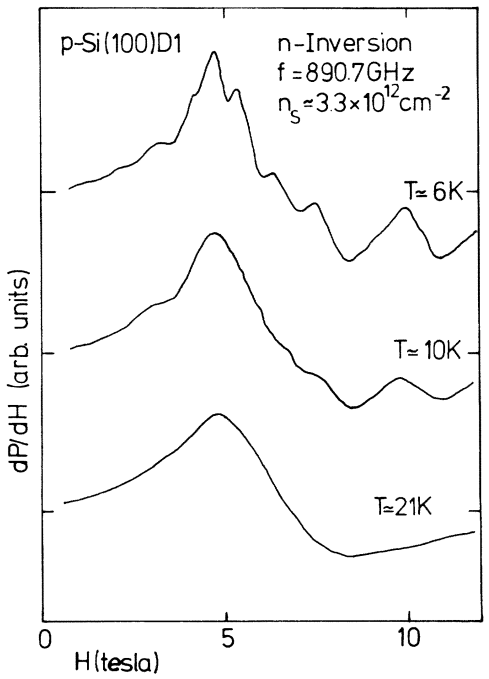

FIG. 8. Temperature dependence of surface CR at high n_s.

cillations can be observed. This is in agreement with Ando's calculations.[9] The high-temperature curves allow a more exacting study of the overall CR line shape, without the perturbation caused by quantum effects. Altogether, the observations on the oscillations show that for $n_s > 1 \times 10^{12}$ cm^{-2} short-range scattering predominates and that Ando's theory gives a good description of the quantum effects.

C. Linewidth and lifetimes

The linewidth of CR in general gives information on the lifetime τ. For an isotropic electron gas with constant τ, the classical description of CR relates the half-width at half-amplitude $\Delta H_{1/2}$ to $\omega\tau$ by

$$\Delta H_{1/2}/H_{\rm res} = 1/\omega\tau \qquad (9)$$

for $\omega\tau \gg 1$. For the two-dimensional electron gas in a high magnetic field this simple classical description is not adequate. The assumption of a constant, field-independent relaxation time τ is not justified. For short-range scatterers the self-consistent Born approximation[9] suggests the relation $\Gamma \propto (\omega_c/\tau_0)^{1/2}$, between the Landau level width parameter Γ and the relaxation time τ_0 in the absence of a field. In as much as the quantum-mechanical calculation gives a width of CR that reflects the Landau-level width at resonance, we are led to expect a proportionality between $1/\tau_{\rm res}$ and $(\omega_c/\tau_0)^{1/2}$. In Fig. 3 we had shown that an approximate fit of the classical conductivity to Ando's results can be used to identify a $\tau_{\rm res}$ and relate it to τ_0. Empirically we establish the relation $1/\omega\tau_{\rm res} = 0.65(1/\omega\tau_0)^{1/2}$. The expression applies at resonance ($\omega_c = \omega$), and is valid for $\omega\tau_{\rm res}$ between 2 and 10. The value of the constant is known only to the accuracy that one can match the classical conductivity to the quantum result. The important point is that one expects a relation of τ_0 and $\tau_{\rm res}$ which is subject to experimental verification.

We have probed the relation for sample $W7$ in a comparison of CR and the microwave-frequency magnetoconductivity. At low frequencies and $\omega_c\tau_0 < 1$, microwave absorption is related to

$$\mathrm{Re}\sigma_{xx}(\omega \to 0, H) = \sigma_0/(1 + \omega_c^2\tau_0^2), \qquad (10)$$

with $\sigma_0 = n_s e^2\tau_0/m_c^*$. Equation (10) gives the field-independent τ_0 as long as $\omega_c\tau_0$ is small. By fitting the variation of the microwave absorption with applied magnetic field, we obtain τ_0. The fit to CR, as discussed in the appendix, gives $\tau_{\rm res}$. In Fig. 9(a) are plotted the values of $1/\tau_{\rm res}$ and $1/\tau_0$ vs n_s. We find that both of these quantities show the generally observed minimum, thought to arise from the two competing scattering mechanisms of charged impurities and surface roughness.[14]

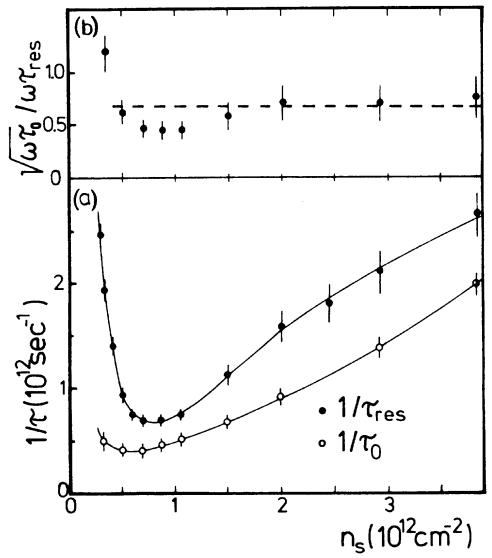

FIG. 9. Comparison of the zero-field scattering rate $1/\tau_0$, with the scattering rate at resonance $1/\tau_{\rm res}$ (sample $W7$, $T \simeq 5$ K). The dashed line in (b) (0.65) is the value predicted for short-range scattering.

$1/\tau_{\rm res}$ is larger than $1/\tau_0$ for all densities n_s. The minimum in $1/\tau_{\rm res}$ appears at somewhat higher n_s, than the corresponding minimum in $1/\tau_0$. With n_s below 0.5×10^{12} cm^{-2}, the CR linewidth and hence $1/\tau_{\rm res}$ increases much more rapidly than $1/\tau_0$. We believe that this is evidence for the onset of inhomogeneous broadening of the resonance. Figure 9(b) gives the ratio $(\omega\tau_0)^{1/2}/\omega\tau_{\rm res}$ as a function of n_s. The dashed line indicates the theoretically predicted constant value 0.65. For $n_s > 1.5 \times 10^{12}$ cm^{-2} there is substantial agreement. The ratio $(\omega\tau_0)^{1/2}/\omega\tau_{\rm res}$ is not only constant, but has the value appropriate for short-range scattering. In the range $0.5 \times 10^{12} \lesssim n_s \lesssim 1.5 \times 10^{12}$ cm^{-2} the ratio is less than the predicted value. This is the density region where Coulomb scattering becomes increasingly important. For very low n_s, below 0.5×10^{12} cm^{-2} in sample $W7$, the ratio again increases as the CR shows evidence for inhomogeneous broadening.

Another, equally significant test of the relation between scattering rates is implied in the frequency scaling experiments.[15,16] One expects $1/\tau_{\rm res}$ to increase as $(\omega)^{1/2}$. Such a tendency has been observed in Refs. 15,16. The $(\omega)^{1/2}$ scaling is expected to be valid for $\omega\tau \gtrsim 2$ and for short-range scattering. With reference to Fig. 9(b), we expect for $n_s > 1.5 \times 10^{12}$ in a sample like $W7$ that this scaling should apply. The work in Ref. 16 makes use of a sample that comes from the same

batch and closely resembles *W7* in its characteristics. Reference 16 finds that at 1.8×10^{12} cm^2 and sufficiently high $\omega\tau$ the $(\omega)^{1/2}$ scaling gives a reasonable description of $1/\tau_{res}$. At densities like 0.7×10^{12} cm^{-2}, where the deviation in Fig. 9(b) is large, there is no evidence for the predicted frequency scaling.

To achieve detailed understanding of the CR linewidth and its relation to the $H=0$ scattering rate, it will be necessary to relate observations such as those in Fig. 9 with frequency and temperature-dependence experiments.

D. Substrate bias experiments

The application of a bias voltage, between a surface contact and the back of the semiconductor substrate, allows one to vary the surface electric field independent of the electron density. The effect of a reverse bias voltage is to increase the surface field, and hence to bind electrons more closely to the surface. The expected result is an increase in the surface roughness scattering rate.[14] A number of interesting observations, related to the application of a bias voltage, have been reported in the recent literature.[17,18]

We have investigated the effect of a reverse substrate bias voltage on CR in an inversion layer on Si(100). The technique for applying the bias voltage to MOS capacitor samples, such as used in these experiments, has been described by Kneschaurek *et al.*[13] The work in Ref. 13 shows explicitly that the length of the depletion layer, and hence depletion charge and surface electric field, is increased with the application of the bias. The effects are documented in low-temperature capacitance-voltage curves, and in their influence on the subband energies. Briefly, the procedure for the bias experiments is the following. We charge the inversion layer at 4.2 °K in the presence of light ($\hbar\omega > \epsilon_g$) to the desired carrier density n_s. The light is then removed, and the gate voltage is raised by the desired amount V_{bias}. Because of a small amount of room-temperature blackbody radiation from the top of the cryostat, the impurity conductivity in the substrate is sufficient to build up the depletion layer to a new, "nonequilibrium" length that relates to the applied bias voltage. The inversion electron density n_s is not changed in the presence of the additional gate voltage. In the time necessary for the experiments (of order several minutes) n_s stays strictly constant as manifested by the unchanged position of the quantum oscillations on the CR (see Figs. 6 and 7).

In Fig. 10 we show a set of experimental curves that is typical for the bias voltage dependence in our samples. The sample is *W7*, and the CR line shape is distorted by interference effects (see Appendix). The data are for a value of n_s near the mobility peak. We observe a marked broadening of the line with the application of V_{bias}. From C-V measurements on similar samples[13] we know that $V_{bias}=-4$ V translates into an increase at the depletion charge density by about 2×10^{11} cm^{-2}.

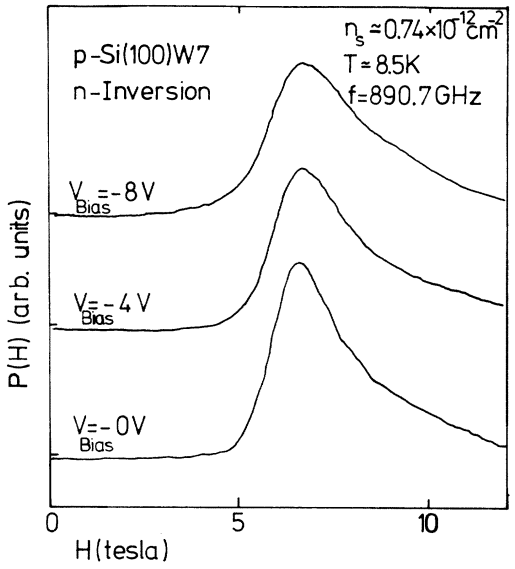

FIG. 10. Dependence of surface CR on substrate bias voltage.

For densities n_s in the range $0.4-2\times10^{12}$ cm^{-2} we find consistently an increased CR linewidth, which we ascribe to increased surface roughness scattering with V_{bias}. The change in $1/\tau_{res}$ is approximately linear with V_{bias} up to -16 V. The slope decreases as n_s is raised. Qualitatively similar results are observed for $1/\tau_0$ in microwave experiments. The effective mass m_c^* stays constant with the decrease of $\omega\tau_{res}$ from 6.5 to 4.4 in Fig. 9. The small shift in the peak position is accounted for by the influence of $\omega\tau$ and interference.

The present results are meant only to qualitatively describe the bias effects in our samples. A more detailed, quantitative evaluation will follow. Our observations are at variance with the very small effects evident in the work of Wagner *et al.*[19] The V_{bias} cited in our experiment must not be compared directly with the V_{sub} quoted in Ref. 19. Because V_{bias} includes the voltage drop across the oxide, $V_{bias} > V_{sub}$ for the same change of the depletion charge. For sample *W7*, the application of $V_{bias}=-4$ V corresponds to a bias of about 2 V across the substrate. The CR broadening that we observe is many times larger than that

reported in Ref. 19. We have not found the decreased scattering that Wagner *et al.* report at $n_s = 0.4 \times 10^{12}$ cm^{-2}. The conflicting results probably arise from differences in the Si-SiO_2 interface of the samples.

E. Subharmonic structure

A wholly unexpected feature of surface CR is the structure that appears on the low-field side of the resonance[6] in Figs. 4 and 7. These peaks have nothing to do with the quantum oscillation. They form approximately a subharmonic sequence H_{res}/n and correspond to $\Delta n = 2, 3, 4$, etc., transitions among the Landau levels. Figure 11 shows the subharmonics at various values of the gate voltage (at 10 V the electron density is approximately 1×10^{12} cm^{-2}). The subharmonics rapidly vanish at densities $n_s < 0.8 \times 10^{-12}$ cm^{-2}. They are observed in both inversion and accumulation layers. In tilt experiments they shift as $(\cos\theta)^{-1}$. They scale with frequency like the fundamental resonance. With increasing temperature they rapidly diminish in amplitude and cannot be observed above $T \sim 20$ °K. The amplitude of $P(H)$ for the $\Delta n = 2$ peak is about 10% of the fundamental at 4.2 K.

The H_{res} identified from the subharmonic sequence lies considerably above the resonance field of the main resonance. In Fig. 12 is plotted nHn vs n_s for $n = 1$, 2, and 3. Here H_n is the field value of the nth absorption maximum. Already at $n_s = 3 \times 10^{12}$ cm^{-3} the subharmonics give a field that lies definitely higher than that of the fundamental. The rise of $n \times H_n$ with decreasing n_s is stronger for $n = 2, 3$ than for the fundamental. Expressed in terms of m_c^*, we get an increase from $0.21 m_0$ to $0.23 m_0$ as n_s decreases from 3×10^{12} to 0.8×10^{12} cm^{-2}. The "subharmonic" mass closely follows the curve that Smith and Stiles[20] have obtained from Shubnikov–de Haas measurements. For comparison that curve has been entered in Fig. 12. The obvious similarity between the two sets of data seems to be more than just accidental.

The existence of subharmonics can be explained in terms of perturbations of the Landau levels. Ando[9] has given a model calculation in which short-range scattering causes a mixing of Landau levels and leads to subharmonic structure in the CR. The experimental observation that the subharmonics vanish at low n_s, where Coulomb scattering predominates, is consistent with this model. In Figs. 3 and 7 the peak at $0.5 H_{res}$ in the theoretical curve is the first subharmonic. Figure 7 makes clear that the experimentally observed peak lies above the calculated result.

The variation of m_c^* with n_s in the Shubnikov–de Haas experiments has been linked to electron-electron interaction effects.[21,22] The observation in Fig. 12 that the "subharmonic" mass follows the Shubnikov–de Haas variation, leads us to sug-

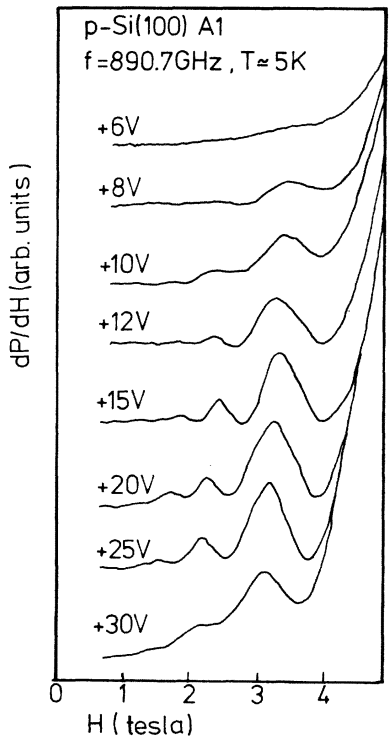

FIG. 11. Subharmonic structure in dP/dH for various gate voltages (at 10 V the electron density is approximately 1×10^{12} cm^{-2}).

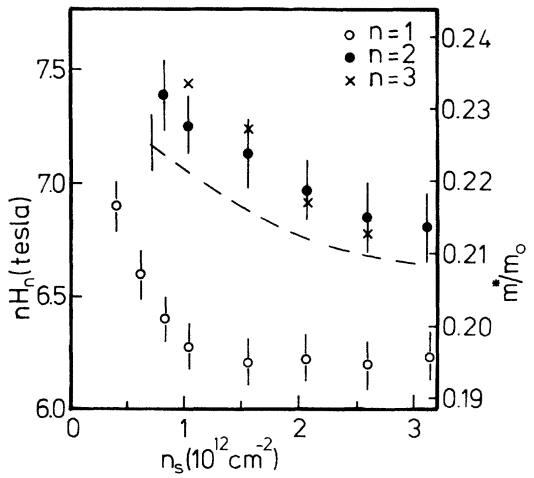

FIG. 12. Plot of the subharmonic fields H_n vs n_s (sample $A1$, $T \simeq 5$ K). The vertical axis gives nH_n, which can be interpreted as a cyclotron mass. The dashed line gives the result of Smith and Stiles (Ref. 20) for the Shubnikov–de Haas mass.

gest that the subharmonics give the interaction enhanced value of m_c^*. This speculation has been confirmed and justified in a recent calculation.[23]

F. Effective mass m_c^*

The precise determination of the cyclotron mass m_c^* requires a careful match of theory to the experimentally observed change of transmitted intensity. Simply marking a transmission minimum is not sufficient. When $n_s > 1\times10^{12}$ cm^{-2}, the quantum oscillation superposed on the signal makes the determination of a resonance field difficult. An important effect, that needs to be accounted for, is interference because of multiple internal reflection in the substrate. The procedure that we have used to identify the mass m_c^*, involves a fit of the transmitted intensity according to the equations given in the appendix. Examples of such a fit are contained in Fig. 18 of the Appendix.

The results for m_c^* are qualitatively different in the high- and low-density limits, with a dividing line which in our samples is $n_s \sim 1\times10^{12}$ cm^{-2}. At high n_s, m_c^* is independent of n_s. At temperatures below 10 K, the value $m_c^* = (0.197 \pm 0.005)m_0$ applies at our experimental frequency 890.7 GHz. Within the quoted uncertainty, this value has been found to be independent of frequency down to 136 GHz.[16] The $\omega\tau$ dependence reported in Ref. 15 was not confirmed in our experiments at 890.7 GHz. Reference 15 cites a variation of m_c^* from 0.193 to $0.220m_0$ as $\omega\tau$ decreases from 5 to 2. No comparable shift in m_c^* has been observed, even though our experiments cover a similar range of $\omega\tau$ between different samples, in substrate bias experiments, and in the variation of τ with n_s above 1×10^{12} cm^{-2}. Our samples do show a marked dependence of m_c^* on temperature.[24]

In the [100] direction of bulk Si, the band-edge mass of the light electrons is known from microwave measurements as $0.1905m_0$ at 4.2 K.[2] Stradling and Zhukov[25] report a small increase of m_c^* with rising temperature, so that at 78 K $m_c^* = (0.199 \pm 0.004)m_0$. The experimental frequency 890.7 GHz corresponds to a thermal energy kT of order 40 K. In order to compare surface and volume values of m_c^* at our far-infrared frequency, we have measured independently the volume resonance of thermally activated electrons at ~ 40 K in an n-type sample. The result is $m_c^* = (0.195 \pm 0.002)m_0$, consistent with the observations in Ref. 25. In Fig. 13 are shown both the volume and surface resonance in one and the same sample for comparison. The surface resonance actually appears at slightly higher field, but within the error limits we conclude that the values coincide.

For $n_s < 10^{12}$ cm^{-2} the behavior is different.

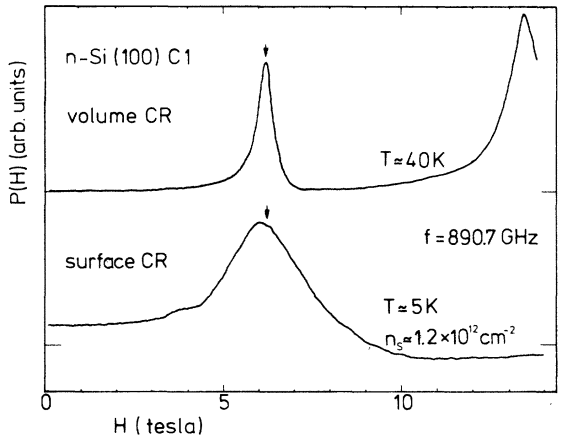

FIG. 13. Volume and surface CR in an n-type Si(100) sample.

Figure 14 shows the dP/dH signal of inversion-layer electrons as a function of n_s. One realizes a definite, unmistakable shift of the resonance position to higher fields as n_s is decreased from 1×10^{12} to 0.4×10^{12} cm^{-2}. We have observed this upward shift in all our samples and in both inversion and accumulation layers. In Fig. 15 the results for different samples are summarized. The rise of the effective mass is as high as 15%. Figure 15 makes clear that the rise of the reso-

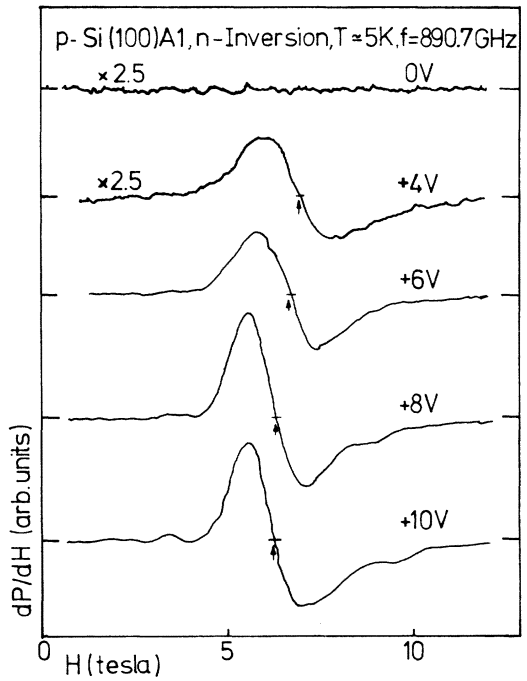

FIG. 14. Surface CR at low electron densities (at 10 V the electron density is approximately 1×10^{12} cm^{-2}). The arrows mark the position of the absorption maximum.

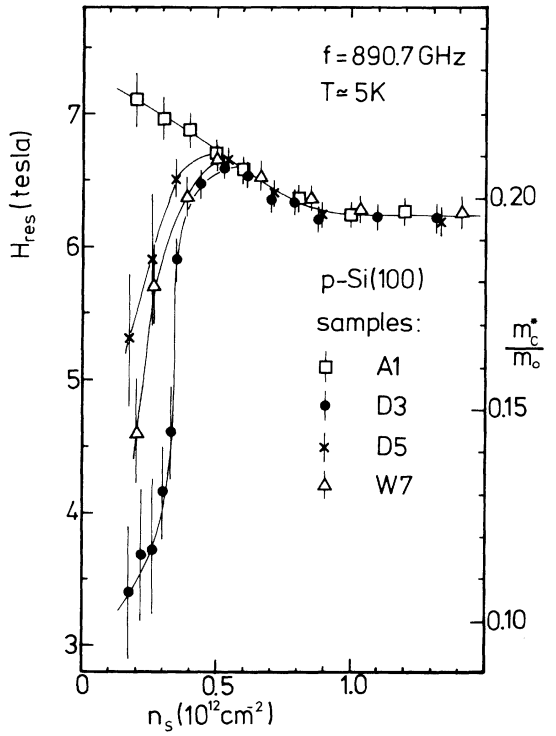

FIG. 15. Resonance fields vs electron density for low values of n_s.

nance field is a universally observed feature, and therefore can sensibly be interpreted as an upward shift of m_c^*. The shift, as shown in Ref. 16, is independent of frequency between 136 and 890.7 GHz. It has been shown to become more pronounced with increasing temperature.[24]

As mentioned in the preceding discussion, a mass increase is expected because of electron-electron interaction effects. An increase has been observed in Shubnikov–de Haas experiments.[20] If one adheres to the general theorems,[26,27] which argue that such interaction cannot be observed in the fundamental CR, one must conclude that at present there is no satisfactory explanation for the shift of m_c^*.

Figure 15 also shows that in some samples, and at the very lowest n_s values, we observe a decrease of the resonance field. This effect has been attributed to electron localization in the fluctuating Si-SiO_2 interface potential.[7,28] In the temperature experiments of Ref. 24, it has been shown that increasing T removes the downward shift. This observation is consistent with the proposed explanation.

G. Electrons in the (110) and (111) surfaces of Si

In addition to experiment on Si(100), we have observed electron CR in inversion and accumulation layers on Si(110) and Si(111). The scattering rate in these samples is larger than for the (100) surface; the $\omega\tau$ is porportionately lower. The expected values of m_c^* are $0.32m_0$ and $0.36m_0$ for (110) and (111) surfaces, respectively.[1]

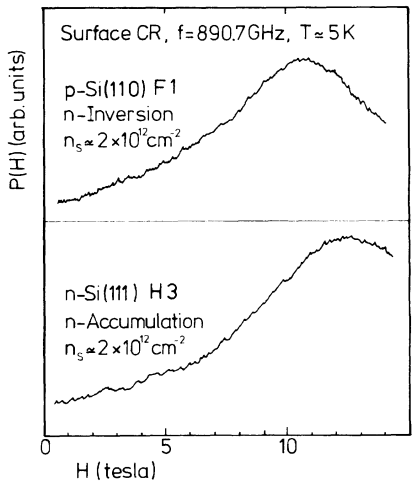

FIG. 16. Surface CR of electrons in the (110) and (111) planes of Si.

Figure 16 shows examples of CR in the two surfaces. Signals were observed for n_s between 1 and 6×10^{12} cm^{-2}. The maximum $\omega\tau$ occurs for $n_s \sim 2\times10^{12}$ cm^{-2} and is about 2.5. Because of the low $\omega\tau$, no subharmonics and quantum oscillations are observed in these traces. The limitation of the magnetic field does not permit us to sweep through the entire resonance line. After fitting the resonance according to the procedure in the Appendix, we derive the values $m^*_{c(110)} = (0.34\pm0.03)m_0$, and $m^*_{c(111)} = (0.38\pm0.03)m_0$. The relatively large uncertainty stems from the low $\omega\tau$, and the fact that the whole CR line is not observed. The values of m_c^* are higher than expected, but still agree within the quoted uncertainty. Recent Shubnikov–de Haas measurements cite[29] $m^*_{c(110)} = (0.38\pm0.03)m_0$ and $m^*_{c(111)} = (0.40\pm0.03)m_0$.

V. CONCLUDING REMARKS

We have demonstrated that CR experiments in space-charge layers on Si yield new information on the electronic properties of the surface electron gas. On the (100) surface of Si many characteristic features of the two-dimensional electron gas have been observed in CR. We conclude that the resonance line shape, the relation of linewidth to the zero-field scattering rate, the quantum oscillations, the localization-induced shift of the resonance, and possibly the subharmonic structure, are adequately explained by theory.[9,10,23,28] As yet unexplained is the upward shift of m_c^* of the

fundamental CR with decreasing n_s. In particular the curious temperature dependence observed for this shift as in Ref. 24 needs attention.

ACKNOWLEDGMENTS

We thank T. Ando for many stimulating discussions related to his calculation and to the interpretation of the experimental results. We are indebted to R. Ranvaud for his help in carrying out experiments at the Hochfeld-Magnetlabor of the Max Planck Institut in Grenoble. We thank the Max Planck Institut for making available their facility to us. The financial support of the Stiftung Volkswagenwerk and the Deutsche Forschungsgemeinschaft (SFB 128) is gratefully acknowledged.

APPENDIX: INTERFERENCE EFFECTS ON THE SURFACE CR LINE SHAPE

Multiple internal reflections in the semiconductor substrate can have a strong influence on the surface CR as observed in transmission. This has recently been recognized by Ortenberg,[30] and Kennedy *et al.*[31] To correct the observed CR line shapes for these interference effects we have calculated the transmission of radiation through a MOS structure consisting of a plane-parallel, nonabsorbing dielectric substrate of refractive index n and thickness d, which on its one face has the space charge layer, an oxide and a semitransparent gate electrode. At first we neglect the influence of the oxide and the gate electrode and consider the space charge layer as an infinitely thin layer of two-dimensional conductivity $\sigma(\omega,H)$. For a two-dimensional electron gas this assumption is justified for normal incidence of radiation of wavelength λ and when λ is large compared to the thickness of the space-charge layer. Using the appropriate boundary conditions we obtain for normal incidence of linearly polarized radiation a power transmission coefficient:

$$T=\tfrac{1}{2}[T(F^{+})+T(F^{-})], \tag{A1}$$

with

$$T(F^{\pm})=16n^2/\left|[(n+1)(n+1+F^{\pm})e^{-ikd} - (n-1)(n-1-F^{\pm})e^{ikd}]\right|^2, \tag{A2}$$

where $F^{\pm}=(4\pi/c)\sigma^{\pm}(\omega,H)=(4\pi/c)(n_s e^2\tau/m_c^{*})S^{\pm}(\omega,H)$ and $k=n\omega/c$. Here $S^{\pm}(\omega,H)$ is the normalized resonance conductivity which is in the classical model given by

$$S^{\pm}(\omega)=[1-i(\omega\mp\omega_c)\tau]^{-1}. \tag{A3}$$

To permit a better comparison to the experimental data we normalize the transmission $T(F)$ in respect to the transmission of the slab at $\sigma^{\pm}=0$ and obtain

$$T_R^{\pm}=\frac{T(F^{\pm})}{T(0)} = \frac{(1-r)^2+4r\sin^2(kd)}{\left|[1+F^{\pm}/(n+1)]e^{-ikd}-r[1-F^{\pm}/(n-1)]e^{+ikd}\right|^2}, \tag{A4}$$

where

$$r=[(n-1)/(n+1)]^2.$$

$T_R=\frac{1}{2}(T_R^{+}+T_R^{-})$ is what is measured in an experiment in which the incident radiation is chopped. The relative change in transmission $P=1-T_R$, which may be called the transmission CR line shape, is measured in an experiment in which the electron density n_s is periodically switched on and off. The transmission Eq. (A4) is a periodic function of sample thickness d with a period of $\lambda/2n$. We therefore characterize samples of thickness d by the dimensionless parameter $y=2nd/\lambda-N$, where N is an integer such that $0\le y<1$. For a frequency of $f=890.7$ GHz ($\lambda=336.6\mu m$) and using the low-temperature refractive index of Si at this frequency $n=3.382$,[32] we obtain $\lambda/2n=49.8\mu m$.

Figure 17 shows the calculated relative transmission T_R for surface CR versus the normalized magnetic field $H/H_{res}=\omega_c/\omega$ at $\omega\tau=5$ and different values of y. Here we have used Eq. (A4) with the classical line shape Eq. (A3). As is evident from Fig. 17 interference effects have a strong influence on the transmission lineshape. The position of the transmission minimum is shifted upwards from $H/H_{res}=1$ for $0<y<0.5$ and downwards for $0.5<y<1.0$. The maximum shifts are obtained for

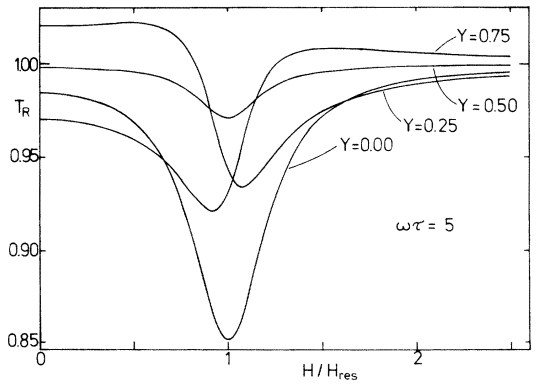

FIG. 17. Relative transmission T_R vs normalized magnetic field H/H_{res} at $\omega\tau=5$ and different values of the interference parameter y. The other parameters used are $f=890.7$ GHz, $n=3.382$, $m^{*}/m_0=0.2$ and $n_s=0.8\times10^{12}$ cm^{-2}.

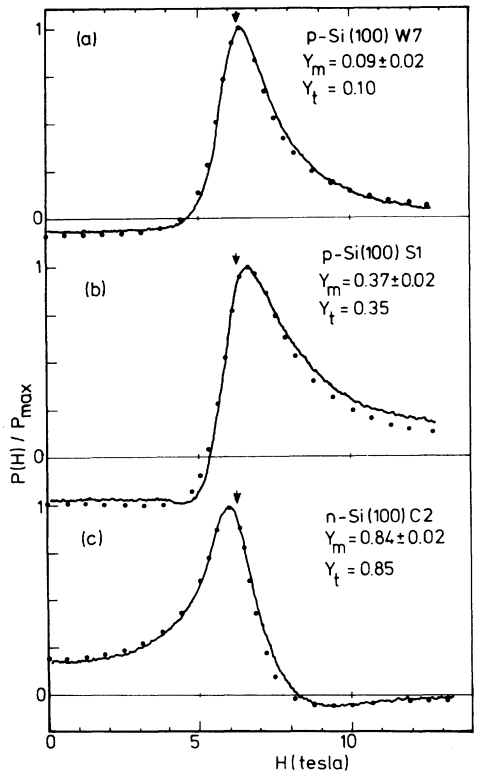

FIG. 18. Measured CR line shapes P/P_{max} vs magnetic field for three samples with different thicknesses at $f = 890.7$ GHz, $T \simeq 5$K, and $n \simeq 1 \times 10^{12}$ cm^{-2}. The dots are a best fit to the data using Eq. (A4); y_t is the value of y used in the fit, while y_m is the value of y determined from the measured thickness of the sample. The fit gives (a) $\omega\tau = 8$, $m_c^*/m_0 = 0.198$, (b) $\omega\tau = 6$, $m_c^*/m_0 = 0.197$, and (c) $\omega\tau = 8$, $m_c^*/m_0 = 0.198$. The resonance fields H_{res} are marked by the arrows.

$y \sim 0.3$ and $y \sim 0.7$, respectively. At a given y the shift of the transmission minimum relative to H/H_{res} depends on $\omega\tau$ and is larger for low $\omega\tau$. For example, for $\omega\tau = 2$ the transmission minimum lies at $H/H_{res} = 1.21$ for $y = 0.3$ and $H/H_{res} = 0.77$ for $Y = 0.7$. For a given y the normalized resonance line shape P/P_{max} depends relatively little on the surface electron density n_s. At high $n_s < 3 \times 10^{12}$ cm^{-2} and $\omega\tau < 5$ the difference to a low n_s lineshape amounts to less than 10% of P_{max} at any value of H/H_{res}.

If we include the effects of the finite oxide of thickness d_{ox} and refractive index n_{ox} and the gate electrode of resistance $R_\square$, we find them to be negligibly small as long as $2d_{ox}n_{ox}/\lambda \lesssim 0.01$ and $R_\square > 377\ \Omega$, conditions which are both satisfied in our experiments.

Figure 18 shows three experimental traces of the normalized line shape P/P_{max} at an electron density of $n_s \simeq 10^{12}$ cm^{-2} for samples with different y. Using our calculation we can reasonably fit the observed line shape and extract from the fit the parameters of interest, i.e., H_{res} and $\omega\tau$. For Figs. 18(a), 18(b), and 18(c) we obtain values of m_c^*/m_0 of 0.198, 0.197, and 0.198, respectively. Note that within experimental accuracy (± 0.005) the values of m_c^*/m_0 are independent of y, the same for inversion layers—Figs. 18(a) and 18(b)—and accumulation layers [Fig. 18(c)], and agree with m_c^*/m_0 determined in volume CR. The typical deviations of the fit from the observed line shape at $H > H_{res}$ are believed to arise from $(H)^{1/2}$ broadening.[9] However, the deviations of the classical fit from the experimental data are sufficiently small to allow interpretation of our data in the presence of interference effects.

---

*Based on a doctoral thesis submitted in partial fulfillment of the requirements for the degree Dr. Rer. Nat.

†Present address: Max-Planck-Institut für Festkörperforschung, Büsnauerstrasse 171, 7 Stuttgart, Germany.

[1]See, for example, G. Dorda, in *Advances in Solid State Physics*, edited by H. J. Qeisser (Pergamon, New York, 1973), Vol. XIII, p. 215; Y. Uemura, in *Proceedings of the 12th International Conference on the Physics of Semiconductors*, edited by M. H. Pilkuhn (Teubner, Stuttgart, 1974), p. 665. F. Stern, CRC Crit. Rev. Solid State Sci. 4, 499 (1974); G. Landwehr, in *Advances in Solid State Physics*, edited by H. J. Qeisser (Pergamon, New York, 1975), Vol. XV, p. 49.

[2]J. C. Hensel, H. Hasegawa, and M. Nakayama, Phys. Rev. 138, 225 (1965).

[3]F. F. Fang, and A. B. Fowler, Phys. Rev. 169, 619 (1968).

[4]G. Abstreiter, P. Kneschaurek, J. P. Kotthaus, and J. F. Koch, Phys. Rev. Lett. 32, 104 (1974).

[5]S. J. Allen, D. C. Tsui, and J. V. Dalton, Phys. Rev. Lett. 32, 107 (1974).

[6]J. P. Kotthaus, G. Abstreiter, and J. F. Koch, Solid State Commun. 15, 517 (1974).

[7]J. P. Kotthaus, G. Abstreiter, J. F. Koch, and R. Ranvaud, Phys. Rev. Lett. 34, 151 (1975).

[8]T. Ando and Y. Uemura, in *Proceedings of the 12th International Conference on the Physics of Semiconductors*, edited by M. H. Pilkuhn (Teubner, Stuttgart, 1974), p. 724.

[9]T. Ando, J. Phys. Soc. Jpn. 38, 989 (1975).

[10]T. Ando, and Y. Uemura, J. Phys. Soc. Jpn. 36, 959 (1974); T. Ando, *ibid.* 36, 1521 (1974); 37, 622 (1974); 37, 1233 (1974).

[11]P. Stallhofer, thesis (TU München, 1975) (unpublished).

[12]G. Dresselhaus, A. F. Kip, and C. Kittel, Phys. Rev. 98, 368 (1955).

[13]P. Kneschaurek, A. Kamgar, and J. F. Koch, Phys. Rev. B 14, 1610 (1976).

[14]See, for example, C. Matsumoto and Y. Uemura, Jpn. J. Appl. Phys. Supp. 2, 367 (1974).

[15]T. A. Kennedy, R. J. Wagner, B. D. McCombe, and D. C. Tsui, Phys. Rev. Lett. 35, 1031 (1975).

[16]G. Abstreiter, J. F. Koch, P. Goy, and Y. Couder, following paper, Phys. Rev. B 14, 2494 (1976).
[17]A. B. Fowler, Phys. Rev. Lett. 34, 15 (1975).
[18]A. A. Lakhani and P. J. Stiles, Solid State Commun. 16, 993 (1975).
[19]R. J. Wagner, T. A. Kennedy, B. D. McCombe, and D. C. Tsui, Surf. Sci. (to be published).
[20]J. L. Smith and P. J. Stiles, Phys. Rev. Lett. 29, 102 (1972).
[21]C. S. Ting, T. K. Lee, and J. J. Quinn, Phys. Rev. Lett. 34, 870 (1975); T. K. Lee, C. S. Ting, and J. J. Quinn, Solid State Commun. 16, 1309 (1975).
[22]B. Vinter, Phys. Rev. Lett. 35, 1044 (1975).
[23]T. Ando, Phys. Rev. Lett. 36, 1383 (1976).
[24]H. Kŭblbeck and J. P. Kotthaus, Phys. Rev. Lett. 35, 1019 (1975).
[25]R. A. Stradling and V. V. Zhukov, Proc. Phys. Soc. Lond. 87, 263 (1966).
[26]E. A. Stern, in *The Fermi Surface*, edited by W. A. Harrison and M. B. Webb (Wiley, New York, 1960).
[27]W. Kohn, Phys. Rev. 123, 1242 (1961).
[28]H. J. Mikeska and H. Schmidt, Z. Phys. 20, 43 (1975).
[29]T. Neugebauer, K. von Klitzing, G. Landwehr, and G. Dorda, Solid State Commun. 17, 295 (1975).
[30]M. von Ortenberg, Solid State Commun. 17, 1335 (1975).
[31]T. A. Kennedy, R. J. Wagner, B. D. McCombe, and J. J. Quinn, Solid State Commun. 18, 275 (1976).
[32]E. V. Loewenstein, D. R. Smith, and R. L. Morgan, Appl. Opt. 12, 398 (1973).